Journal of Materials Chemistry C

RSC Publishing

PAPER

Intelligent display films with tunable color emission based on a supermolecular architecture†

Cite this: *J. Mater. Chem. C*, 2013, **1**, 5654

Rui Tian,[a] Ruizheng Liang,[a] Dongpeng Yan,[a] Wenying Shi,[a] Xuejiao Yu,[a] Min Wei,*[a] Lin Song Li,*[b] David G. Evans[a] and Xue Duan[a]

Received 11th June 2013
Accepted 18th July 2013

DOI: 10.1039/c3tc31119h

www.rsc.org/MaterialsC

Multi-color emission materials (especially white light) have broad applications in optoelectronics, light-emitting diodes (LEDs) and optical devices. This work describes the fabrication of multicolor and white-light-emitting ultrathin films (UTFs) with 2D architecture based on CdTe quantum dots (QDs: red or green emission), an organic chromophore (BTBS: blue emission) and MgAl layered double hydroxide (LDH) nanosheets *via* the layer-by-layer assembly method. The hybrid UTFs possess a periodic long-range ordered layered structure, which is verified by X-ray diffraction. By rational selection of the building unit and control of the assembly sequence, the luminescence color of the resulting UTFs can be precisely tuned throughout the whole visible-light region. Especially, finely controlled white-light emission was successfully achieved with the color coordinates at (0.322, 0.324), rather close to the standard coordinates of white light (0.333, 0.333). In addition, the QDs–BTBS–LDH UTF displays intelligent photoluminescence behavior, *i.e.*, white, orange, or red emission can be obtained for the same UTF by changing the excitation light. Therefore, this work provides a facile approach for accurate fabrication of multi-color/white-light photoemission UTFs, which is expected to be used in full-color displays, sensing and intelligent response.

Introduction

Multi-color emission materials[1–7] (especially white-light emission[8–11]) have been intensively studied as excellent candidates in bioimaging, illumination, microlasers and light emitting diodes (LEDs). Conventional strategies to develop multiplexed emission generally rely on combination of three primary color (red, green and blue) luminescence species (*e.g.*, organic dyes and rare-earth compounds).[9–12] Although extensive progress has been made, several problems remain not well-resolved for these materials. For instance, the low luminous efficiency of organic dyes,[12] and deficiency in full-color display of rare-earth compounds[13] severely affects their fluorescence behavior. Recently, quantum dots (QDs) have been investigated as promising candidates in photonic and optoelectronic devices,[8,14–17] due to their excellent properties including high quantum yields, good stability, wide excitation spectrum and high spectral purity.[18–20] However, bright, color-saturated blue QDs are rather rare owing to the expensive and complicated synthesis process, which restricts the development of full-color displays.[21] Therefore, how to achieve multi-color emission materials with the advantages of high purity and color saturation throughout the whole visible-light region still remains a challenging goal.

To date, several methods have been explored to fabricate multi-color emission films or devices, including spin-coating,[22] baking[23] and vacuum thermal deposition,[24] but these conventional route generally suffer from a lack of uniformity, low efficiency, or aggregation-led quenching.[15,25,26] Consequently, it is highly essential to develop new materials or approaches for the fabrication of multi- and white-color emission with largely improved luminescence performance. Layered double hydroxides (LDHs), whose structure can be expressed by the general formula $[M_{1-x}^{II}M_x^{III}(OH)_2]^{z+}A^{n-}_{z/n}\cdot yH_2O$ (M^{II} and M^{III} are divalent and trivalent metal ions respectively and A^{n-} is an anion), are one important type of inorganic layered material which possess high stability and versatility in chemical composition.[27–36] The LDHs can be exfoliated into positively charged monolayers that serve as building blocks for constructing various 2D-organized functional nanocomposites *via* layer-by-layer (LBL) techniques, which have been particularly investigated in fluorescence films.[37–41] In our previous work, we reported the single- and multi-color ultrathin films based on LBL assembly of LDH monolayers and organic chromophores.[41,42] However, the fluorescence intensity and precise

[a]*State Key Laboratory of Chemical Resource Engineering, Beijing University of Chemical Technology, Beijing 100029, P. R. China. E-mail: weimin@mail.buct.edu.cn; Fax: +86-10-64425385; Tel: +86-10-64412131*

[b]*Key Laboratory for Special Functional Materials, Henan University, Kaifeng 475004, P. R. China. E-mail: lsli@henu.edu.cn*

† Electronic supplementary information (ESI) available: UV-vis absorption spectra, CIE 1931 color coordinates, morphological and structural characterization and fluorescence lifetime of the multi-color/white UTFs. See DOI: 10.1039/c3tc31119h

control of multi-color emission (especially white color) are still not satisfactory. This inspires us to fabricate superior multi-color films by combination of QDs with organic chromophores into an LDH layered matrix, so as to take the advantages of both counterparts: (i) the incorporation of QDs and organic chromophores would achieve high purity, color saturation and favorable brightness; (ii) the multi-color and especially white-light emission can be finely tailored throughout the whole visible-light region, by virtue of the versatile single-color unit as well as the facile assembly process.

In this work, we demonstrate the fabrication of multi-color ultrathin films (UTFs) *via* LBL assembly of LDH nanosheets with green- and red-emitting CdTe QDs (defined as QD-530: emission at ~530 nm in solution with particle size of ~2.5 nm; QD-620: emission at ~620 nm in solution with particle size of ~4.0 nm) and a blue-emitting organic compound, 2,2′-(1,2-ethenediyl)bis-[5-[[4-(diethylamino)-6-[(2,5-disulfophenyl)amino]-1,3,5-triazin-2-yl]amino]benzenesulfonic acid] hexasodium salt (BTBS, illustrated in Scheme 1). The as-prepared UTFs display a periodic long-range ordered structure and high dispersion of chromophores within the LDH interlayer microenvironment. Based on rational selection of the building units and control of the assembly sequence, the color emission of UTFs can be precisely tuned throughout the whole visible-light region; especially, finely controlled white-light emission was successfully achieved. These sophisticated UTFs exhibit largely improved fluorescence intensity, brightness and stability. In addition, the QDs–BTBS–LDH hybrid UTF displays intelligent photoluminescence behavior, *i.e.*, white, orange, or red emission can be obtained for the same UTF by changing the excitation light.

Results and discussion

In order to fabricate heterogeneous multi-color luminescent UTFs, we employed the stepwise LBL assembly of individual luminescent species and LDH nanosheets. Scheme 1 shows the detailed assembly process of the multi-color UTFs system, which involves the tuning of chromophore, assembly sequence and bilayer number. With the purpose of achieving multi-color UTFs with high purity and color saturation, the independent emission of each individual chromophore is rather important. In our previous work,[37] we have found Fluorescence Resonance Energy Transfer (FRET) would occur within 13.94 nm between CdTe QD-530 (green emission at ~530 nm in solution) and QD-620 (red emission at ~620 nm in solution). In an effort to inhibit possible FRET between adjacent photo-active species, inert poly(sodium *p*-styrenesulfonate) (PSS) units were assembled as spacers between two kinds of chromophore bilayers to exclude the occurrence of FRET, so as to obtain independent emission. We illustrate several multi-color as well as white-color emission UTFs in the following section.

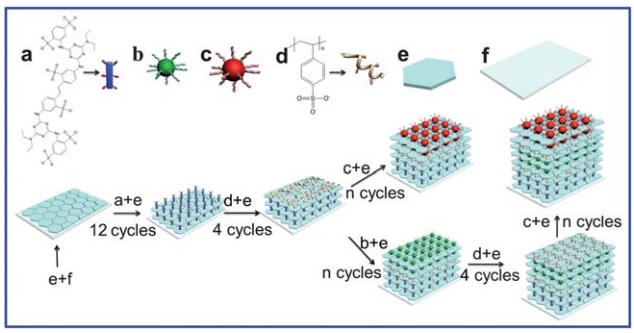

Scheme 1 Schematic representation for the LBL fabrication of multilayer luminous UTFs: (a) BTBS (blue luminescence), (b) QD-530 (green luminescence; particle size: ~2.5 nm), (c) QD-620 (red luminescence; particle size: ~4.0 nm), (d) PSS, (e) LDH nanosheet and (f) quartz glass substrate.

Assembly of mono-color luminescence UTFs

Serving as a primary color resource, the single blue (BTBS), green (QD-530) and red (QD-620) units were assembled with LDH nanosheets as described in our previous work (see details in Fig. S1, S2, Table S1†).[37,43] Fig. 1 displays the fluorescence emission spectra of $(BTBS/LDH)_n$ UTFs (λ_{em}: 440 nm), $(QD\text{-}530/LDH)_n$ UTFs (λ_{em}: 533 nm) and $(QD\text{-}620/LDH)_n$ UTFs (λ_{em}: 630 nm), with a linear enhancement of maximal emission which can be visually confirmed by their photographs under UV-light irradiation (Fig. 1, insets). Additionally, the $(BTBS/LDH)_{30}$, $(QD\text{-}530/LDH)_{30}$ and $(QD\text{-}620/LDH)_{30}$ UTFs show bright blue, green and red color with photoluminescence quantum yields (PLQY) of 9.7%, 10.6% and 5.8% respectively, which make them good building units for the fabrication of multi-color UTFs.

Assembly of multi-color luminescent UTFs

Blue/green color emission. In order to achieve a gradual color change from blue towards green, we carried out the fabrication process by assembling QD-530/LDH units onto the as-prepared $(BTBS/LDH)_{12}$ for finely tunable photo-emission.

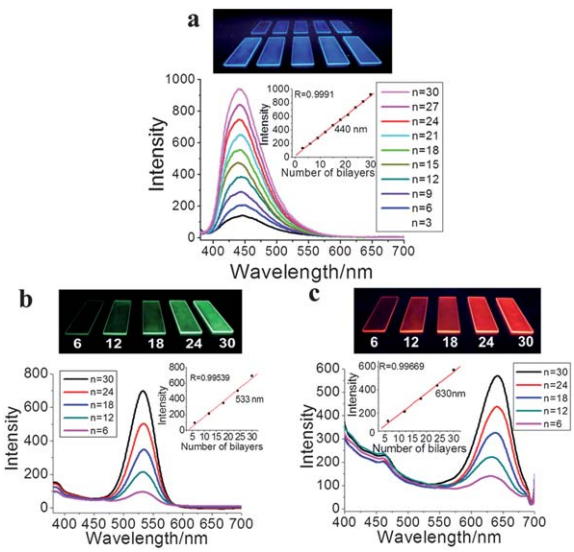

Fig. 1 Fluorescence spectra and photographs of UTFs under UV irradiation (365 nm): (a) $(BTBS/LDHs)_n$ UTFs (n = 3–30), (b) $(QD\text{-}530/LDH)_n$ UTFs (n = 6–30), (c) $(QD\text{-}620/LDH)_n$ UTFs (n = 6–30). The insets show the fluorescence intensity as a function of n.[37,43] The particle sizes of QD-530 and QD-620 are ~2.5 nm and ~4.0 nm, respectively.

The multilayer assembly process of the $(BTBS/LDH)_{12}(QD\text{-}530/LDH)_n$ UTFs was monitored by UV-vis absorption spectroscopy, in which the absorption intensity at ~500 nm attributed to QD-530 increases linearly along with the bilayer number n (Fig. S3†), indicating an ordered and uniform deposition procedure. Fig. 2a displays the florescence spectra of these UTFs: the emission peak at 440 nm is attributed to the $(BTBS/LDH)_{12}$ unit; while the one at 533 nm is due to the $(QD\text{-}530/LDH)_n$ unit. It is observed that the peak intensity at 533 nm shows a monotonic increase with the increase of bilayer number of (QD-530/LDH) units. The gradual change in luminescence can be seen from photographs under UV illumination (Fig. 2b). The color coordinate measurement CIE (Commission Internationale de l'Eclairage)[44] demonstrates that the luminescence color can be tuned from blue (Table S2: CIE 1931: (0.159, 0.108); $n = 0$)† to greenish blue (CIE 1931: (0.179, 0.254); $n = 8$), and then to bluish green (CIE 1931: (0.219, 0.376); $n = 20$) by simply changing the bilayer number of the green unit QD-530/LDH (CIE 1931: (0.228, 0.503)) (Fig. 2c). Therefore, a gradient change from blue to green can be achieved by assembly of QD-530/LDH units onto the surface of $(BTBS/LDH)_{12}$ UTF.

Blue/red color emission. The assembly process for B/R bicolor luminescence involves the deposition of $(QD\text{-}620/LDH)_n$ ($n = 0$–20) units onto the as-prepared $(BTBS/LDH)_{12}$ UTF, which was monitored by UV-vis absorption spectroscopy (Fig. S4†). The fluorescence intensity at 630 nm shows gradual enhancement upon increasing bilayer number (Fig. 3a), indicating the uniform growth of film assembly. The fluorescence spectra of these UTFs show no obvious emission shift in comparison with the pristine BTBS/LDH and QD-620/LDH UTFs (Fig. 1), which excludes the possibility of interaction or aggregation between luminescence species. The photographs of these UTFs under UV illumination (Fig. 3b) provide a visual verification of the strong luminescent brightness. The color coordinate measurements reveal that the luminescence color of the UTFs changes from blue (Table S3: CIE 1931: (0.159, 0.108); $n = 0$)† to purplish blue (CIE 1931: (0.179, 0.123); $n = 2$), purple (CIE 1931: (0.245, 0.144); $n = 4$), reddish purple (CIE 1931: (0.377, 0.207); $n = 12$) and finally to purplish red (CIE 1931: (0.477, 0.255); $n = 20$) in sequence (Fig. 3c), by simply increasing the bilayer number of the red unit QD-620/LDH (CIE 1931: (0.589, 0.310)). As a result, this method achieves finely tunable UTFs with strong luminescent brightness and attractive color chromaticity.

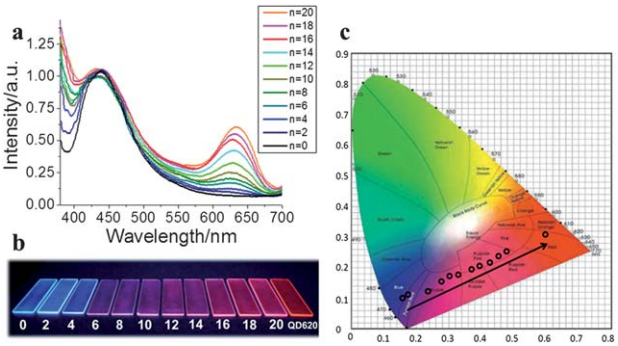

Fig. 3 Optical spectroscopy characterization of the $(BTBS/LDH)_{12}(QD\text{-}620/LDH)_n$ ($n = 0$–20) UTFs: (a) fluorescence spectra, (b) their photographs under UV light (365 nm) irradiation as well as the pristine $(QD\text{-}620/LDH)_{20}$ UTF, (c) variation in the color coordinates with the increase of n.

Assembly of white-color luminescent UTFs

White-color emission. We further carried out the fabrication of white-color UTFs by using the blue, green and red building units. In this case, the (QD-620/LDH) bilayer unit was deposited onto the surface of as-prepared $(BTBS/LDH)_{12}(QD\text{-}530/LDHs)_{16}$ UTF (Scheme 1) and the whole process was monitored by UV-vis absorption spectroscopy (Fig. S5†). In the fluorescence spectra of the $(BTBS/LDH)_{12}(QD\text{-}530/LDHs)_{16}(QD\text{-}620/LDHs)_n$ UTFs, the emission peaks at 440, 533 and 630 nm corresponding to the (BTBS/LDH), (QD-530/LDH) and (QD-620/LDH) units, respectively (Fig. 4a), show no obvious shift in the maximum photoemission compared with the individual pristine building units. The gradual enhancement of peak intensity at ~630 nm confirms the uniform growth and progressive color change across the white region, which is visually shown in Fig. 4b. The luminescent color of these UTFs varies from bluish green ($(BTBS/LDH)_{12}(QD\text{-}530/LDHs)_{16}(QD\text{-}620/LDHs)_1$ with CIE 1931: (0.228, 0.382)) through the white region, finally to pink ($(BTBS/LDH)_{12}(QD\text{-}530/LDHs)_{16}(QD\text{-}620/LDHs)_{12}$ with CIE 1931: (0.407,

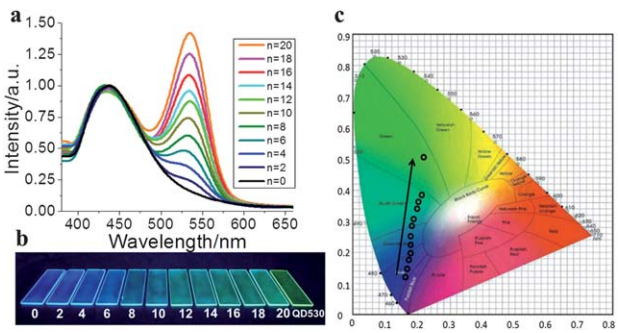

Fig. 2 Optical spectroscopy characterization of the $(BTBS/LDH)_{12}(QD\text{-}530/LDH)_n$ ($n = 0$–20) UTFs: (a) fluorescence spectra, (b) their photographs under UV light (365 nm) irradiation as well as the pristine $(QD\text{-}530/LDH)_{20}$ UTF, (c) variation in the color coordinates with the increase of n.

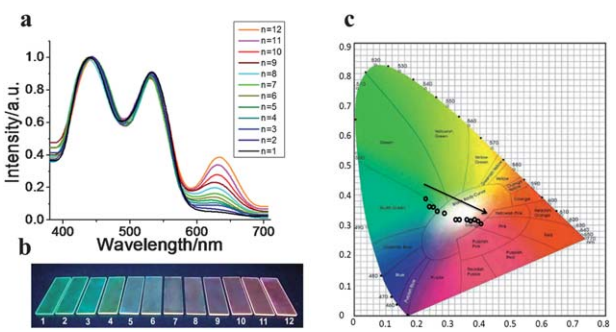

Fig. 4 Optical spectroscopy characterization of the $(BTBS/LDH)_{12}(QD\text{-}530/LDH)_{16}(QD\text{-}620/LDH)_n$ ($n = 1$–12) UTFs: (a) fluorescence spectra, (b) their photographs under UV light irradiation (365 nm), (c) variation in the color coordinates with the increase of n.

0.308)) (see Fig. 4c and Table S4†). In particular, the luminescent color of the $(BTBS/LDH)_{12}(QD\text{-}530/LDHs)_{16}(QD\text{-}620/LDHs)_n$ ($n = 5$–8) UTFs passes through the white-light region of the CIE 1931 diagram.

Precisely controlled white-color emission. The achievement of precisely controlled white color is important, owing to its wide use in displays and lighting, especially for the purposes of energy conservation and simplification of equipment.[45–48] By adjusting the deposition sequence and relative ratio of the BTBS/LDH, QD-530/LDH and QD-620/LDH units, luminescent UTFs with finely tunable photo-emission in the white spectral region were obtained. The detailed fabrication sequence and optical characteristics of luminescence UTFs are shown in Fig. 5. The color coordinates (Fig. 5A) show a very precisely controlled variation in photoemission in the white color region, based on careful tuning of the relative content of each mono-color unit (Fig. 5C), which are visualized in the photographs (Fig. 5B). Finally, we found that the $(BTBS/LDH)_{12}(QD\text{-}530/LDH)_{16}(QD\text{-}620/LDH)_7$ UTF (denoted as f in Fig. 5C) shows the best white-light emission, and its color coordinates (0.322, 0.324) are rather close to the standard coordinates of white light (0.333, 0.333). In order to give a further insight into the merits of this assembly method, the photoluminescence behavior of a drop-cast film was studied as a comparison sample, which shows inhomogeneous fluorescence, color distortion and impurity (Fig. S6A†). This is attributed to the aggregation-led red-shift and quenching (Fig. S6B†) as a result of the disordered structure. Therefore, we have demonstrated the idea of achieving white-light emission with high purity and strong brightness *via* precise control of the mono-color assembly.

Intelligent fluorescence UTFs

Intelligent materials, which can recognize external stimuli and produce a definite response, are promising in many applications including sensing, health monitoring and multi-functionality.[49–52] Based on the responses to external excitation light *via* the alteration of emission color, fluorescent materials have been intensively investigated in the areas of anti-forgery, colorimetric sensors and display devices.[46,53] In this work, we demonstrate the white-color UTF as an intelligent photo-luminescence material which gives different emission colors in response to different excitation light. According to the UV-vis absorption spectra of these three chromophores (Fig. S2†) as well as the wide excitation spectrum of QDs, it is suggested that BTBS can be effectively excited at 360 nm while QD-530 and QD-620 can be excited by photon energies above 500 and 600 nm, respectively. This motivates us to explore the different emissions in the presence of different excitation wavelengths. As shown in Fig. 6, the $(BTBS/LDH)_{12}(QD\text{-}530/LDH)_{20}$ $(QD\text{-}620/LDH)_7$ UTF displays three different emission spectra as well as corresponding white, orange and red color, with the excitation light of 360, 460 and 560 nm, respectively. When excited at 360 nm, the UTF exhibits emissions at 440, 533 and 630 nm, which generates white light as a consequence. The excitation light of 460 nm produces the emission peaks at 533 and 630 nm, which results in orange light to the naked eye. In the case of excitation light of 560 nm, only 630 nm emission was observed

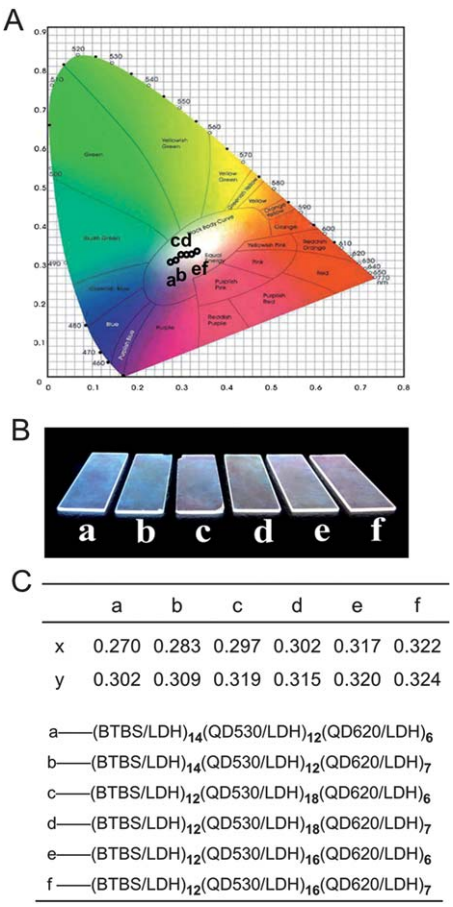

Fig. 5 Optical spectroscopy characterization of the $(BTBS/LDH)_m$ $(QD\text{-}530/LDH)_n(QD\text{-}620/LDH)_p$ UTFs: (A) the change in color coordinates in the white-light region, (B) their photographs under UV light (365 nm), (C) the color coordinates and detailed compositions of these UTFs.

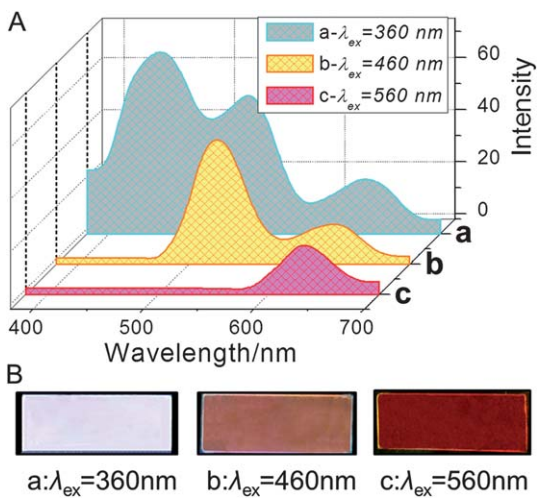

Fig. 6 (A) The emission spectra, (B) photographs (taken under an RFPC light source) of the $(BTBS/LDH)_{12}(QD\text{-}530/LDH)_{20}(QD\text{-}620/LDH)_7$ UTF with different excitation wavelengths: (a) excited at 360 nm, (b) excited at 460 nm, (c) excited at 560 nm.

with red color display. In particular, the strong emission of white, orange and red color can be visually and directly observed by the naked eye without the assistance of any instrument. Therefore, the $(BTBS/LDH)_{12}(QD\text{-}530/LDH)_{20}(QD\text{-}620/LDH)_7$ UTF exhibits tunable white, orange and red emission as a response towards the variation of excitation light, which is expected to show potential uses in optical devices including colorimetric sensors, photonic switches and multiband filters.[54]

Structural and morphological characterization

The structural and morphological properties of these UTFs were further studied. The small angle XRD patterns of the mono-color UTFs (Fig. S7†) display the basal reflection at $2\theta \sim 5.71^\circ$, 1.91° and 1.29° for $(BTBS/LDH)_{30}$, $(QD\text{-}530/LDH)_{30}$ and $(QD\text{-}620/LDH)_{30}$ UTF, respectively, indicating a periodic long-range ordered superlattice structure of these UTFs with a repeating thickness of 1.55, 4.62 and 6.80 nm. Additionally, the periodic structure of the multi-color luminescent UTFs was also verified (Fig. 7a). For instance, in the XRD pattern of $(BTBS/LDH)_{12}(QD\text{-}530/LDH)_{16}(QD\text{-}620/LDH)_{12}$ UTF (Fig. 7, a3), reflections at 2θ 1.26° and 1.9° were observed, corresponding to the basal spacing of 4.65 and 7.01 nm associated with the superlattice structures of QD-530/LDH and QD-620/LDH unit, respectively. The reflection of the BTBS/LDH unit is rather weak (Fig. S7A†) and therefore was not observed. Similar results were also obtained for the $(BTBS/LDH)_{12}(QD\text{-}530/LDH)_{20}$ and $(BTBS/LDH)_{12}(QD\text{-}620/LDH)_{20}$ systems (Fig. 7a, Table S5†). The surface morphology of $(BTBS/LDH)_{12}(QD\text{-}530/LDH)_{20}$ (B/G), $(BTBS/LDH)_{12}(QD\text{-}620/LDH)_{20}$ (B/R) and $(BTBS/LDH)_{12}(QD\text{-}530/LDH)_{16}(QD\text{-}620/LDH)_{12}$ (B/G/R) UTFs was investigated by SEM and AFM. The top-view SEM images (Fig. S8A–S10A†) display the homogeneity of these UTFs upon increasing bilayer number n, and typical SEM images for B/G, B/R and B/G/R UTFs are shown in Fig. 7b. The AFM topographical images (2 μm × 2 μm) of the multi-color UTFs are illustrated in Fig. 7C and S8B–S10B,† with the root-mean square roughnesses of 5.977, 6.321 and 8.364 nm for the B/G, B/R and B/G/R UTFs respectively (Table S6†), indicating the continuous and smooth surface of these UTFs. The UTF thickness can be estimated from their side-view SEM images (Fig. S8C–S10C†), from which an approximately linear increase of film thickness as a function of n was observed. Average thickness increments of 1.72, 4.58 and 6.40 nm per bilayer cycle were obtained for BTBS/LDH, QD-530/LDH and QD-620/LDH units, respectively (Table S6†), which is consistent with the XRD observations (1.55, 4.62 and 6.80 nm). The results further confirm the uniform and periodic layered structure of these UTFs throughout the fabrication process.

Stability

Photo- and storage stability are of great significance for multi-emission materials, which would severely influence their applications in photonic or optoelectronic devices. Photostability test was carried out by illuminating the LBL assembled UTFs with UV light, in comparison with the drop-cast film which was prepared by simply dropping the mixed chromophores solution onto the surface of quartz glass followed by drying at room temperature. For the drop-cast film after 5 h irradiation, the PL intensities at 440, 533 and 630 nm decreased to 56.2%, 60.5% and 67.8% of their original values, respectively (Fig. S11A†). However, Fig. 8a displays the fluorescence intensity changes at 440, 533 and 630 nm in the $(BTBS/LDH)_{12}(QD\text{-}530/LDH)_{16}(QD\text{-}620/LDH)_7$ UTF as a function of bleaching time, from which 71.4%, 75.6% and 78.1% of the original intensities were maintained under the same test conditions. The results demonstrate that the LBL assembled UTFs possess a better UV-resistance capability by employment of the LDH matrix.

In addition, the storage stability test shows that ~98% of its initial fluorescence intensity remained (Fig. 8b) after three months of measurement, in contrast to ~89% (Fig. S11B†) for the drop-cast film with the same measurement. The influence of humidity was also investigated, and no obvious change in fluorescence intensity was observed with relative humidity values of 30% and 70% (Fig. S12†). Moreover, by fitting the decay profiles, the fluorescence lifetimes were obtained. Compared with the mono-color UTFs, the emission lifetimes of

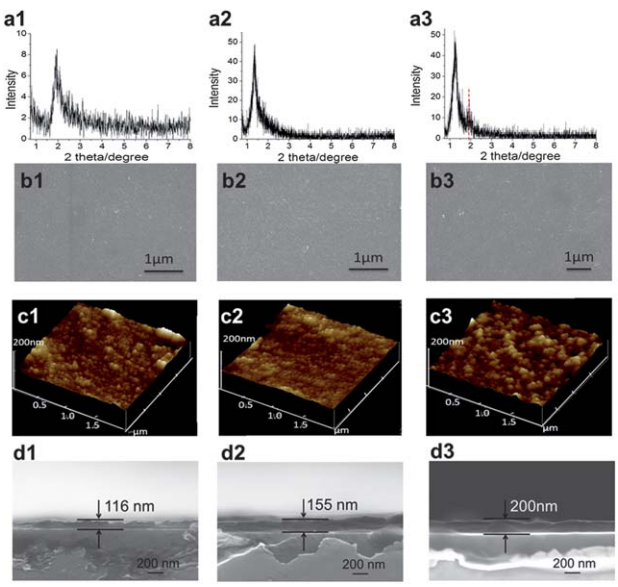

Fig. 7 The structural and morphological characterization of $(BTBS/LDH)_{12}(QD\text{-}530/LDH)_{20}$, $(BTBS/LDH)_{12}(QD\text{-}620/LDH)_{20}$ and $(BTBS/LDH)_{12}(QD\text{-}530/LDH)_{16}(QD\text{-}620/LDH)_{12}$ UTFs: (a) XRD patterns, (b) top-view SEM images, (c) tapping-mode AFM topographical images, (d) side-view SEM images.

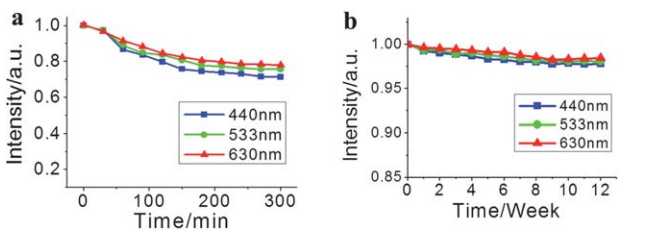

Fig. 8 (a) Photostability of the $(BTBS/LDH)_{12}(QD\text{-}530/LDH)_{16}(QD\text{-}620/LDH)_7$ UTF upon irradiation by UV light (365 nm) for 300 min; (b) the fluorescence intensity of the $(BTBS/LDH)_{12}(QD\text{-}530/LDH)_{16}(QD\text{-}620/LDH)_7$ UTF (stored at room temperature) recorded weekly for 3 months.

multi-color and white-color UTFs at 440, 533 and 630 nm become longer (Table S7†), which can be attributed to the interaction between the chromophore and the rigid LDH nanosheets. Therefore, it is concluded that the LDH nanosheets provide a rigid and confined 2D microenvironment for the ordered and uniform dispersion of chromophores, resulting in the largely enhanced stability and prolonged fluorescence lifetime.

Conclusions

In summary, ordered luminous UTFs were fabricated by effective assembly of inorganic LDH nanosheets with organic BTBS molecules and QDs on quartz substrates. The UTFs exhibit a periodic long-range heterogeneous structure, uniform morphology and controllable film thickness on the nanometer scale. The luminescence color of the resulting hybrid UTFs can be easily tuned over the whole visible-light spectrum, specifically for precisely regulated white emission, by rational control of the R/G/B color photoemissive building blocks as well as their sequence. The fluorescent intensity, photostability and storage stability are remarkably enhanced due to the immobilization of chromophores within the interlayer region of LDH nanosheets. Moreover, the B/G/R UTF displays intelligent photoluminescence behavior which gives different emission colors (white, orange, red) in response to different excitation light. It is anticipated that this facile and cost-effective strategy for accurately tuned multi-color and white-light emission would facilitate potential applications in displays, lasers and optoelectronic devices.

Acknowledgements

This work was supported by the National Natural Science Foundation of China (NSFC), the 973 Program (Grant no. 2011CBA00504) and the Collaboration Project from the Beijing Education Committee. M. Wei particularly appreciates the financial aid from the China National Funds for Distinguished Young Scientists of the NSFC.

Notes and references

1 V. Wood, M. J. Panzer, J. Chen, M. S. Bradley, J. E. Halpert, M. G. Bawendi and V. Bulović, *Adv. Mater.*, 2009, **21**, 2151.
2 J. Kwak, W. K. Bae, D. Lee, I. Park, J. Lim, M. Park, H. Cho, H. Woo, Y. Yoon do, K. Char, S. Lee and C. Lee, *Nano Lett.*, 2012, **12**, 2362.
3 M. Shang, D. Geng, X. Kang, D. Yang, Y. Zhang and J. Lin, *Inorg. Chem.*, 2012, **51**, 11106.
4 Y. Zhang, G. Li, D. Geng, M. Shang, C. Peng and J. Lin, *Inorg. Chem.*, 2012, **51**, 11655.
5 A. A. Zakhidov, J.-K. Lee, J. A. DeFranco, H. H. Fong, P. G. Taylor, M. Chatzichristidi, C. K. Ober and G. G. Malliaras, *Chem. Sci.*, 2011, **2**, 1178.
6 Q. Liu, J. Peng, L. Sun and F. Li, *ACS Nano*, 2011, **5**, 8040.
7 Y. Yang, Q. Zhao, W. Feng and F. Li, *Chem. Rev.*, 2013, **113**, 192.
8 W. Ki and J. Li, *J. Am. Chem. Soc.*, 2008, **130**, 8114.
9 Z. Y. Mao and D. J. Wang, *Inorg. Chem.*, 2010, **49**, 4922.
10 T. E. Rosson, S. M. Claiborne, J. R. McBride, B. S. Stratton and S. J. Rosenthal, *J. Am. Chem. Soc.*, 2012, **134**, 8006.
11 T. Sheng, Z. Fu, X. Wang, S. Zhou, S. Zhang and Z. Dai, *J. Phys. Chem. C*, 2012, **116**, 19597.
12 J. Xu, J. Liang, J. Li and W. Yang, *Langmuir*, 2010, **26**, 15722.
13 W. R. Liu, C. H. Huang, C. W. Yeh, J. C. Tsai, Y. C. Chiu, Y. T. Yeh and R. S. Liu, *Inorg. Chem.*, 2012, **51**, 9636.
14 S. Kim, T. Kim, M. Kang, S. K. Kwak, T. W. Yoo, L. S. Park, I. Yang, S. Hwang, J. E. Lee, S. K. Kim and S. W. Kim, *J. Am. Chem. Soc.*, 2012, **134**, 3804.
15 A. H. Mueller, M. A. Petruska, M. Achermann, D. J. Werder, E. A. Akhadov, D. D. Koleske, M. A. Hoffbauer and V. I. Klimov, *Nano Lett.*, 2005, **5**, 1039.
16 F. Qian, S. Gradecak, Y. Li, C. Y. Wen and C. M. Lieber, *Nano Lett.*, 2005, **5**, 2287.
17 M. Lee, R. Yang, C. Li and Z. L. Wang, *J. Phys. Chem. Lett.*, 2010, **1**, 2929.
18 P. O. Anikeeva, J. E. Halpert, M. G. Bawendi and V. Bulovic, *Nano Lett.*, 2007, **7**, 2196.
19 L. Kim, P. O. Anikeeva, S. A. Coe-Sullivan, J. S. Steckel, M. G. Bawendi and V. Bulovic, *Nano Lett.*, 2008, **8**, 4513.
20 A. B. Greytak, P. M. Allen, W. Liu, J. Zhao, E. R. Young, Z. Popović, B. J. Walker, D. G. Nocera and M. G. Bawendi, *Chem. Sci.*, 2012, **3**, 2028.
21 Z. Tan, F. Zhang, T. Zhu, J. Xu, A. Y. Wang, J. D. Dixon, L. Li, Q. Zhang, S. E. Mohney and J. Ruzyllo, *Nano Lett.*, 2007, **7**, 3803.
22 W. K. Bae, J. Kwak, J. Lim, D. Lee, M. K. Nam, K. Char, C. Lee and S. Lee, *Nano Lett.*, 2010, **10**, 2368.
23 S. Jeong, J. Lee, J. Nam, K. Im, J. Hur, J.-J. Park, J.-M. Kim, B. Chon, T. Joo and S. Kim, *J. Phys. Chem. C*, 2010, **114**, 14362.
24 E. n. Ishow, A. Brosseau, G. Clavier, K. Nakatani, P. Tauc, C. l. Fiorini-Debuisschert, S. Neveu, O. Sandre and A. Léaustic, *Chem. Mater.*, 2008, **20**, 6597.
25 J. S. Bendall, M. Paderi, F. Ghigliotti, N. Li Pira, V. Lambertini, V. Lesnyak, N. Gaponik, G. Visimberga, A. Eychmüller, C. M. S. Torres, M. E. Welland, C. Gieck and L. Marchese, *Adv. Funct. Mater.*, 2010, **20**, 3298.
26 J. Y. Woo, K. Kim, S. Jeong and C.-S. Han, *J. Phys. Chem. C*, 2011, **115**, 20945.
27 Q. Wang and D. O'Hare, *Chem. Rev.*, 2012, **112**, 4124.
28 M. Darder, M. López-Blanco, P. Aranda, F. Leroux and E. Ruiz-Hitzky, *Chem. Mater.*, 2005, **17**, 1969.
29 G. R. Williams, A. M. Fogg, J. Sloan, C. Taviot-Gueho and D. O'Hare, *Dalton Trans.*, 2007, 3499.
30 G. R. Williams and D. O'Hare, *J. Mater. Chem.*, 2006, **16**, 3065.
31 X. L. Liu, M. Wei, Z. L. Wang, D. G. Evans and X. Duan, *J. Phys. Chem. C*, 2008, **112**, 17517.
32 A. M. Fogg, A. J. Freij and G. M. Parkinson, *Chem. Mater.*, 2002, **14**, 232.
33 L. Li, R. Ma, Y. Ebina, N. Iyi and T. Sasaki, *Chem. Mater.*, 2005, **17**, 4386.

34 G. Abellán, E. Coronado, C. Martí-Gastaldo, A. Ribera and J. F. Sánchez-Royo, *Chem. Sci.*, 2012, **3**, 1481.
35 S. Si, A. Taubert, A. Mantion, G. Rogez and P. Rabu, *Chem. Sci.*, 2012, **3**, 1945.
36 W. Shi, S. He, M. Wei, D. G. Evans and X. Duan, *Adv. Funct. Mater.*, 2010, **20**, 3856.
37 R. Liang, S. Xu, D. Yan, W. Shi, R. Tian, H. Yan, M. Wei, D. G. Evans and X. Duan, *Adv. Funct. Mater.*, 2012, **22**, 4940.
38 Z. Li, J. Lu, S. Li, S. Qin and Y. Qin, *Adv. Mater.*, 2012, **24**, 6053.
39 F. Leroux and C. Taviot-Guého, *J. Mater. Chem.*, 2005, **15**, 3628.
40 L. Desigaux, M. B. Belkacem, P. Richard, J. Cellier, P. Leone, L. Cario, F. Leroux, C. Taviot-Gueho and B. Pitard, *Nano Lett.*, 2006, **6**, 199.
41 D. Yan, J. Lu, J. Ma, M. Wei, D. G. Evans and X. Duan, *Angew. Chem., Int. Ed.*, 2011, **50**, 720.
42 D. Yan, J. Lu, M. Wei, S. Qin, L. Chen, S. Zhang, D. G. Evans and X. Duan, *Adv. Funct. Mater.*, 2011, **21**, 2497.
43 D. Yan, J. Lu, M. Wei, S. Li, D. G. Evans and X. Duan, *Phys. Chem. Chem. Phys.*, 2012, **14**, 8591.
44 T. Schwaebel, O. Trapp and U. H. F. Bunz, *Chem. Sci.*, 2013, **4**, 273.
45 L. Zhu and Y. Zhao, *J. Mater. Chem. C*, 2013, **1**, 1059.
46 M. S. Wang, S. P. Guo, Y. Li, L. Z. Cai, J. P. Zou, G. Xu, W. W. Zhou, F. K. Zheng and G. C. Guo, *J. Am. Chem. Soc.*, 2009, **131**, 13572.
47 C. Vijayakumar, K. Sugiyasu and M. Takeuchi, *Chem. Sci.*, 2011, **2**, 291.
48 P. Audebert and F. Miomandre, *Chem. Sci.*, 2013, **4**, 575.
49 M. in het Panhuis, *J. Mater. Chem.*, 2006, **16**, 3598.
50 S. R. Mukti and C. D. Bakul, *Adv. Mater.*, 2002, **14**, 443.
51 P. Hilgers, A. Riechers and B. König, *Angew. Chem., Int. Ed.*, 2008, **47**, 3089.
52 R. Yoshida, *Adv. Mater.*, 2010, **22**, 3463.
53 M. Yoshida and J. Lahann, *ACS Nano*, 2008, **2**, 1101.
54 Y. J. Kang, J. Walish and E. L. Thomas, U. S. Pat, 0086208A1, 2009.

